

An Improved Control Method for a DFIG in a Wind Turbine under an Unbalanced Grid Voltage Condition

Sol-Bin Lee*, Kyo-Beum Lee[†], Dong-Choon Lee** and Jang-Mok Kim***

Abstract – This paper presents a control method, which reduces the pulsating torque and DC voltage problems of a doubly fed induction generator (DFIG)-based wind turbine system. To reduce the torque and power ripple, a current control scheme consisting of a proportional integral (PI) controller is presented in a positive synchronously rotating reference frame, which is capable of providing precise current control for a rotor-side converter with separated positive and negative components. The power theory can reduce the oscillation of the DC-link voltage in the grid-side converter. In this paper, the generator model is examined, and simulation results are obtained with a 3 kW DFIG-based wind turbine system to verify the proposed control strategy.

Keywords: Doubly fed induction generator, Unbalanced disturbance, Torque oscillation, DC voltage ripple, Power generation control, Power theory

1. Introduction

Wind energy has become one of the fastest growing renewable energy systems in the world today. Thus, the demand for the connection of large-scale wind parks to the power grid is on the rise. Many large-scale wind parks employ the doubly fed induction generator (DFIG) with variable speed wind turbines. The main advantages of DFIG wind turbine systems are the four-quadrant active and reactive power controls and the small converter size [1].

Wind turbine systems are installed in remote rural areas with good wind resources. However, the distribution systems in these areas are usually unbalanced because many wind turbines are connected in weak areas where there are heavy unsymmetrical loads, transitory faults, voltage dips, unsymmetrical transformer windings, or transmission impedances. The unbalanced voltages on the grid side converter may produce a large voltage ripple in the DC-link voltage and result in unequal non-sinusoidal output currents, unequal heating, and power losses. These unbalanced voltages may also shorten the lifetime of the DC capacitors in the grid-connected wind turbines with DFIG. A very small unbalanced voltage can create a large unbalanced current. These effects can cause an oscillation of the torque and power in the generator that can, in turn, lead to speed pulsations, acoustic noise, increased losses, and shorter insulation life [2]-[6].

The instantaneous oscillation of the three phase active power produces the oscillation in the DC-link voltage. The

oscillation component has a frequency band, which is twice that of the grid frequency. Based on symmetrical components analysis, the interaction of the different sequence components of the balanced and unbalanced grid voltages and currents can lead to torque oscillation.

Many control methods that reduce the pulsating torque and the DC-link voltage have been introduced in the literature. In [7], the DFIG under unbalanced conditions use a feed-forward loop on the field-oriented current controller to limit the torque ripple; this is simple and robust. In [8], the DFIG under an unbalanced condition use a separate control of the positive and negative of the rotor current, with an additional negative sequence control loop to reduce the pulsating torque and the reactive power. However, the GSC dynamics are not considered.

This paper proposes a control method for the DFIG under unbalanced grid voltages. The main purpose is to reduce the torque oscillation and the DC-link voltage for the control of both the rotor-side converter (RSC) and the grid-side converter (GSC). The RSC controls the positive and negative components of the rotor current independently to reduce the torque oscillations through a dual controller. However, the power oscillation in a stator and a rotor cannot be controlled simultaneously. The ripple of the DC-link voltage occurs with the difference between the power of the rotor side and the power flowing into the grid through the GSC. To make the power of the grid and the rotor equal, power theory is adopted to reduce the ripple of the DC-link voltage in the GSC control. This paper presents a control strategy, which improves the control of the DFIG under an unbalanced grid voltage condition. A proposed control strategy, based on the dual controller and power theory, is developed to attain these objectives. The generator model is examined in this paper, and the simulation results are obtained using a 3 kW DFIG-based wind turbine system to verify the proposed control strategy.

* Corresponding Author: School of Electrical and Computer Engineering, Ajou University, Korea. (kyl@ajou.ac.kr)

† School of Electrical and Comp. Engineering, Ajou University, Korea. (sgaeng@ajou.ac.kr)

** Department of Electrical Engineering, Yeungnam University, Korea. (dclee@yu.ac.kr)

*** Department of Electrical Engineering, Pusan National University, Korea. (jmok@pusan.ac.kr)

2. The Wind Turbine Generator System

The DFIG is a wound rotor induction motor with stator windings that are directly connected to the grid. The RSC controls the active and reactive powers of the DFIG independently. The GSC is used to regulate the DC-link voltage between the two converters, and its power factor is usually set to unity. Various control strategies are used to achieve this. The most popular of these is aligning the d axis of the GSC currents abc to the d - q transformation along a reference frame linked to the grid voltage. Therefore, the DC-link voltage regulator output reference current becomes oriented along this d axis to supply or absorb the active power from the grid [9]-[10]. A schematic diagram for the DFIG is shown in Fig. 1.

2.1 The Modeling of the DFIG

The DFIG d - q model in an arbitrary reference frame is expressed as follows:

$$\mathbf{V}_s = R_s \mathbf{I}_s + \frac{d\lambda_s}{dt} + j\omega \lambda_s, \quad (1)$$

$$\mathbf{V}_r = R_r \mathbf{I}_r + \frac{d\lambda_r}{dt} + j(\omega - \omega_r) \lambda_r, \quad (2)$$

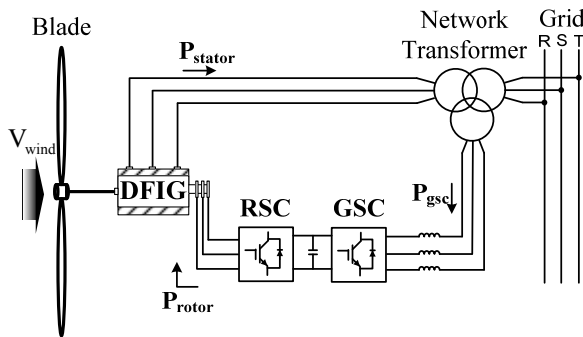


Fig. 1. The schematic for the DFIG system.

$$\lambda_s = \lambda_{ds} + j\lambda_{qs}, \quad \lambda_r = \lambda_{dr} + j\lambda_{qr}, \quad (3)$$

$$\lambda_{ds} = L_s I_{ds} + L_m I_{dr}, \quad \lambda_{qs} = L_s I_{qs} + L_m I_{qr} \quad (4)$$

and

$$\lambda_{dr} = L_r I_{dr} + L_m I_{ds}, \quad \lambda_{qr} = L_r I_{qr} + L_m I_{qs}, \quad (5)$$

where I_{ds} , I_{qs} , I_{dr} , and I_{qr} are the currents of the stator and rotor in d and q -axes, respectively; λ_{ds} , λ_{qs} , λ_{dr} , and λ_{qr} are the fluxes of the stator and rotor in d and q -axes, respectively; R_s and R_r are the resistances of the stator and rotor windings, respectively; and ω_r is the rotor speed.

According to (3) and (5), the rotor flux and stator current can be expressed using the stator flux and rotor current as:

$$\lambda_r = \left(\frac{L_m}{L_s} \right) \lambda_s + \sigma L_r \mathbf{I}_r, \quad \mathbf{I}_s = \frac{(\lambda_s - L_m \mathbf{I}_r)}{L_s}, \quad (6)$$

where $\sigma = 1 - L_m^2 / (L_r L_s)$ is the leakage factor.

Under an unbalanced supply, the stator and rotor voltage, current, and flux contain both positive and negative components. A convenient way to model a DFIG is to use a positive reference frame rotating at the speed of ω_s and a negative reference frame rotating at the speed of $-\omega_s$. Fig. 2 shows that the $d+$ axis is fixed to the positive stator flux and rotates at the speed of ω_s , where the $d-$ axis rotates at an angular speed of $-\omega_s$, with the phase angle to the α -axis being $-\theta_s$.

The positive and negative components are detected by a low pass filter, a notch filter, a band pass filter, and a delay signal cancellation [11]. The delay signal cancellation method was used in this paper because of its very exact and fast characteristics. When the α - β frame is fixed on the grid voltage, the positive and negative components can be described as shown in (7) as:

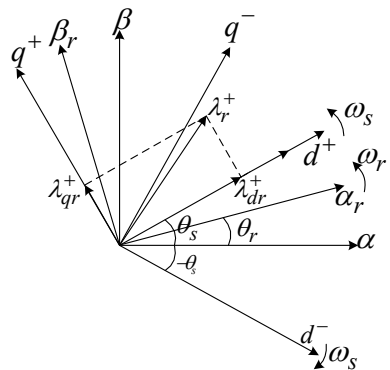


Fig. 2. The relationship between the $\alpha\beta$, $dq+$ and the $dq-$ reference frames.

$$\begin{bmatrix} v_\alpha(t) \\ v_\beta(t) \\ v_\alpha(t-T/4) \\ v_\beta(t-T/4) \end{bmatrix} = \begin{bmatrix} v^P \cos(\omega t + \theta) + v^n \cos(-\omega t + \theta) \\ v^P \cos(\omega t + \theta) + v^n \cos(-\omega t + \theta) \\ v^P \sin(\omega t + \theta) - v^n \sin(\omega t + \theta) \\ v^n \cos(-\omega t + \theta) - v^P \cos(\omega t + \theta) \end{bmatrix}, \quad (7)$$

where T is the period of the fundamental frequency.

The positive and negative components can be described as shown in (8):

$$\begin{bmatrix} v_\alpha^P(t) \\ v_\beta^P(t) \\ v_\alpha^n(t) \\ v_\beta^n(t) \end{bmatrix} = \frac{1}{2} \begin{bmatrix} 1 & 0 & 0 & -1 \\ 0 & 1 & 1 & 0 \\ 1 & 0 & 0 & 1 \\ 0 & 1 & -1 & 0 \end{bmatrix} \begin{bmatrix} v_\alpha(t) \\ v_\beta(t) \\ v_\alpha(t-T/4) \\ v_\beta(t-T/4) \end{bmatrix}. \quad (8)$$

The positive and negative sequences in the stationary α - β reference frame can be further transformed into positive d - q and negative d - q sequences using:

$$\begin{bmatrix} v_d^p(t) \\ v_q^p(t) \\ v_d^n(t) \\ v_q^n(t) \end{bmatrix} = \begin{bmatrix} \cos\theta & \sin\theta \\ -\sin\theta & \cos\theta \\ \cos(-\theta) & \sin(-\theta) \\ -\sin(-\theta) & \cos(-\theta) \end{bmatrix} \begin{bmatrix} v_\alpha^p(t) \\ v_\beta^p(t) \\ v_\alpha^n(t) \\ v_\beta^n(t) \end{bmatrix}. \quad (9)$$

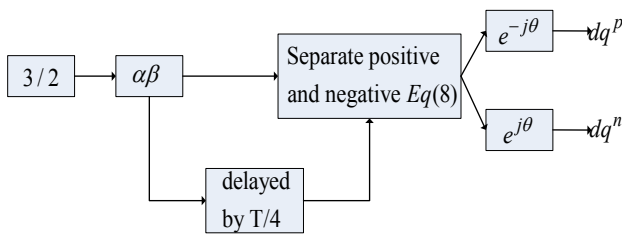


Fig. 3. The separated positive and negative sequences.

At the moment of the voltage dip and the recovery, the separated positive and negative sequences are summarized (Fig. 3).

2.2 Power and Torque of the DFIG

The power and the torque of the DFIG in the reference frame based on the stator field can be described as shown in (10) and (11):

$$S = P_s + jQ_s = \frac{3}{2} V_s^e \times I_s^{e*} \quad (10)$$

and

$$T_e = \frac{3}{2} \frac{P}{2} \frac{L_m}{L_s} (\lambda_{qs}^e i_{dr}^e - \lambda_{ds}^e i_{qr}^e). \quad (11)$$

However, when the grid voltage is unbalanced, the total stator field is distorted into an ellipse by the positive and negative components of the field. Given that the field has maximum and minimum values twice in one period, rippling with a frequency band that is twice the line frequency appears in the power and the torque.

3. The RSC and GSC Control Methods of the DFIG System

3.1 The Rotor-side Converter

The stator power under an unbalanced grid voltage condition can be obtained in (12) and (13). This model provides a basis for system optimization, such as the minimization of the torque or power oscillations using RSC [12]–[14] expressed as

$$P_s = P_{s0} + P_s \sin 2 \sin(2\theta_s t) + P_s \cos 2 \cos(2\theta_s t) \quad (12)$$

and

$$Q_s = Q_{s0} + Q_s \sin 2 \sin(2\theta_s t) + Q_s \cos 2 \cos(2\theta_s t), \quad (13)$$

where

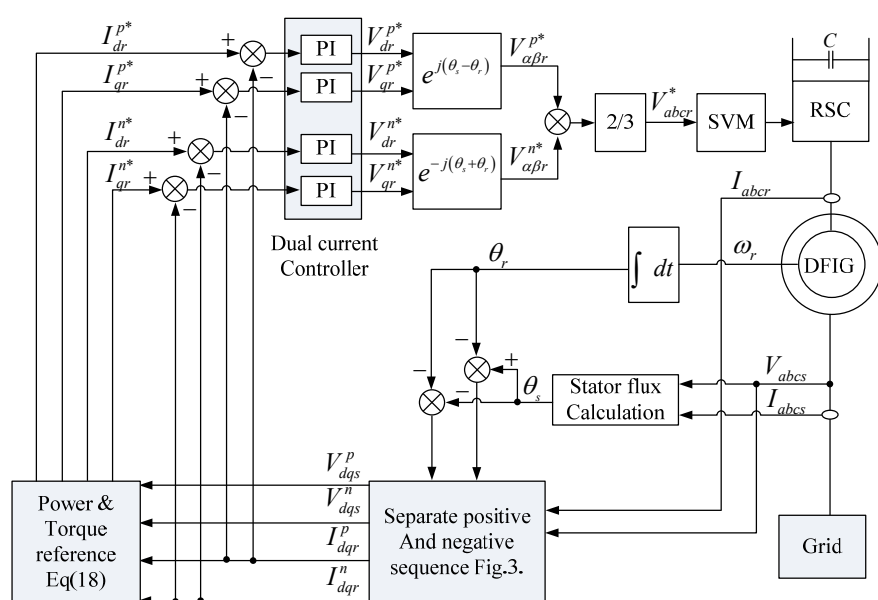


Fig. 4. The schematic block diagram of the proposed strategy in RSC.

$$\begin{bmatrix} P_{s0} \\ P_{scos2} \\ P_{ssin2} \\ Q_{s0} \\ Q_{scos2} \\ Q_{ssin2} \end{bmatrix} = \begin{bmatrix} v_{ds}^p & v_{qs}^p & v_{ds}^n & v_{qs}^n \\ v_{ds}^n & v_{qs}^n & v_{ds}^p & v_{qs}^p \\ v_{ds}^n - v_{qs}^n - v_{ds}^p & v_{qs}^p & i_{ds}^p \\ v_{qs}^p - v_{ds}^p & v_{qs}^n - v_{ds}^n & i_{qs}^p \\ v_{qs}^n - v_{ds}^n & v_{qs}^p - v_{ds}^p & i_{ds}^n \\ -v_{sd}^n - v_{qs}^n & v_{ds}^p & v_{qs}^p \end{bmatrix} \begin{bmatrix} i_{ds}^p \\ i_{qs}^p \\ i_{ds}^n \\ i_{qs}^n \end{bmatrix}. \quad (14)$$

Here, (14) expresses the active and reactive powers in the stator side, both of which have the oscillation parts. The oscillation parts of the active and reactive powers cause a ripple in the DC-link voltage and torque pulsation. To limit the ripple of the DC-link voltage or the torque pulsation under an unbalanced grid voltage, the oscillation of the active and reactive powers in the stator has to be controlled to zero.

The electromagnetic power under an unbalanced grid voltage condition is described as:

$$P_e = \frac{3}{2} \frac{L_m \omega_r}{L_s} (P_{e0} + P_{esin2} \sin(2\theta_s t) + P_{ecos2} \cos(2\theta_s t)), \quad (15)$$

where

$$\begin{bmatrix} P_{e0} \\ P_{ecos2} \\ P_{esin2} \end{bmatrix} = \begin{bmatrix} -v_{ds}^p - v_{qs}^p & v_{ds}^n & v_{qs}^n \\ v_{qs}^n - v_{ds}^n & v_{qs}^p - v_{ds}^p & i_{dr}^p \\ v_{ds}^n & v_{qs}^n - v_{ds}^p - v_{qs}^p & i_{qr}^n \end{bmatrix} \begin{bmatrix} i_{dr}^p \\ i_{qr}^p \\ i_{dr}^n \\ i_{qr}^n \end{bmatrix}. \quad (16)$$

The electromagnetic torque of the DFIG is calculated as:

$$T_e = \frac{P_e}{\left(\frac{\omega_r}{n}\right)}, \quad (17)$$

where n is the number of pole pairs.

The electromagnetic torque has a ripple, which is twice of the grid frequency. In (16), the torque and the active power of the stator can be reduced into i_{drp} , i_{qrp} , i_{drn} , and i_{qrn} . To reduce torque ripple, P_{ecos2} and P_{esin2} have to be controlled by the rotor current control to make them equal to '0.' To control the power and to keep the power factor as '1,' the P_{e0} has to be the power reference and the current reference of the rotor to make the reactive power zero. The current reference of rotor can be described as:

$$\begin{bmatrix} i_{dr}^p \\ i_{qr}^p \\ i_{dr}^n \\ i_{qr}^n \end{bmatrix} = \begin{bmatrix} v_{ds}^p & v_{qs}^p & v_{ds}^n & v_{qs}^n \\ v_{ds}^p - v_{qs}^p & v_{ds}^n - v_{qs}^n & & \\ v_{qs}^n - v_{ds}^n & v_{qs}^p - v_{ds}^p & & \\ v_{ds}^n & v_{qs}^n - v_{ds}^p - v_{qs}^p & & \end{bmatrix}^{-1} \begin{bmatrix} P_{e0} \\ Q_{s0} \\ P_{ecos2} \\ P_{esin2} \end{bmatrix}. \quad (18)$$

Consequently, the oscillations of the power and torque can be reduced using i_{drp} , i_{qrp} , i_{drn} , and i_{qrn} in the RSC. Fig. 4 shows the schematic block diagram of the proposed strategy in RSC.

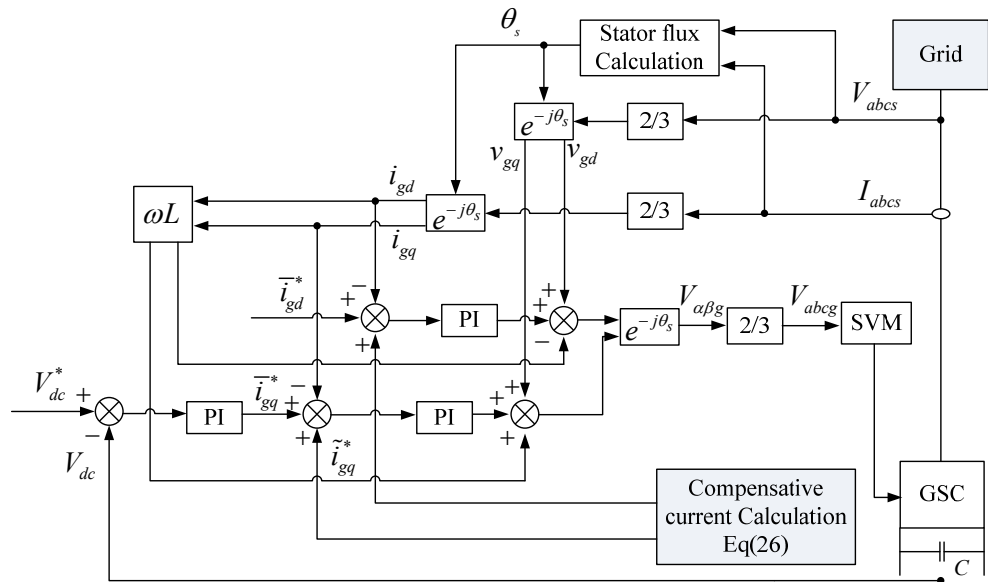


Fig. 5. The schematic block diagram of the proposed strategy in GSC.

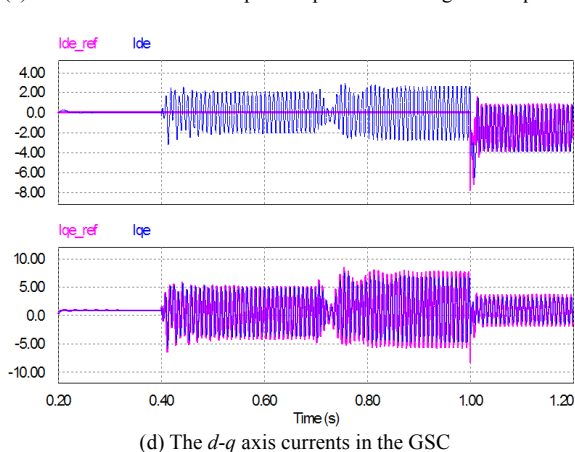
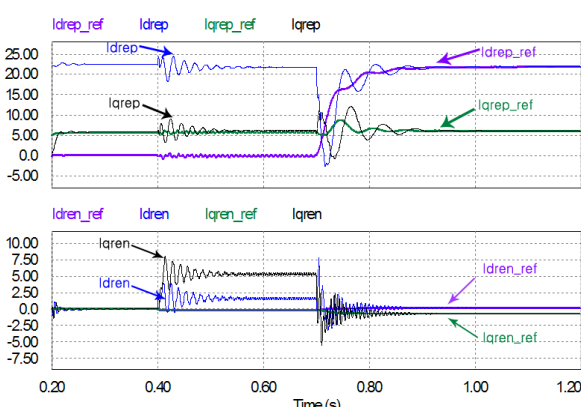
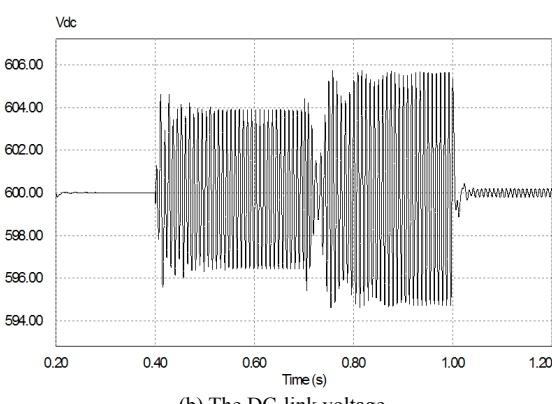
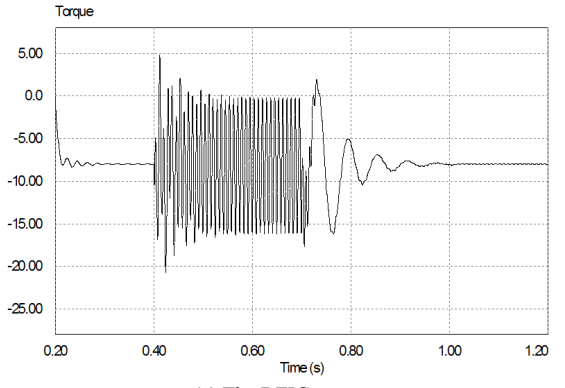


Fig. 6. The simulation results applied to the proposed strategy.

3.2 The Grid-side Converter

The DC-link voltage is obtained by [15]:

$$C \frac{dV_{dc}}{dt} = \frac{P_g}{V_{dc}} - \frac{P_r}{V_{dc}}, \quad (19)$$

where

$$P_g = P_{g0} + P_g \sin 2 \sin(2\theta_e t) + P_g \cos 2 \cos(2\theta_e t) \quad (20)$$

$$\begin{aligned} P_r &= P_s - P_e \\ &= P_{s0} - P_{e0} + (P_s \sin 2 - P_e \sin 2) \sin(2\theta_e t) \\ &\quad + (P_s \cos 2 - P_e \cos 2) \cos(2\theta_e t). \end{aligned} \quad (21)$$

According to (20) and (21):

$$C \frac{dV_{dc}}{dt} V_{dc} = (P_{g0} - P_{r0}) + (\tilde{P}_{g0} - \tilde{P}_{r0}), \quad (22)$$

where

$$\tilde{P}_{g0} = P_g \sin 2 \sin(2\theta_e t) + P_g \cos 2 \cos(2\theta_e t) \quad (23)$$

and

$$\tilde{P}_{r0} = P_r \sin 2 \sin(2\theta_e t) + P_r \cos 2 \cos(2\theta_e t). \quad (24)$$

The oscillation of the DC-link voltage can be described by (23) and (24) as:

$$C \frac{d\tilde{V}_{dc}}{dt} V_{dc} = (\tilde{P}_{g0} - \tilde{P}_{r0}). \quad (25)$$

To reduce the rippling of the DC-link voltage, models P_g and P_r must be similar. If the ripple of the active power of RSC and GSC is controlled to zero, the DC-link voltage has no oscillation. However, the rotor power has an oscillation because the RSC is controlled to reduce the torque ripple. Therefore, the GSC should be controlled to have the same value as the oscillation in the active power. The compensative currents are shown in (26) using the power theory found in [16]:

$$\begin{bmatrix} \tilde{i}_{gd_comp} \\ \tilde{i}_{gq_comp} \end{bmatrix} = \begin{bmatrix} v_{gd} & v_{gq} \\ -v_{gq} & v_{gd} \end{bmatrix}^{-1} \begin{bmatrix} \tilde{P}_{g0} - \tilde{P}_{r0} \\ \tilde{Q}_{g0} - \tilde{Q}_{r0} \end{bmatrix}. \quad (26)$$

The compensative currents reduce the ripple of the DC-link voltage through control input. Fig. 5 shows the compensative block diagram in the GSC.

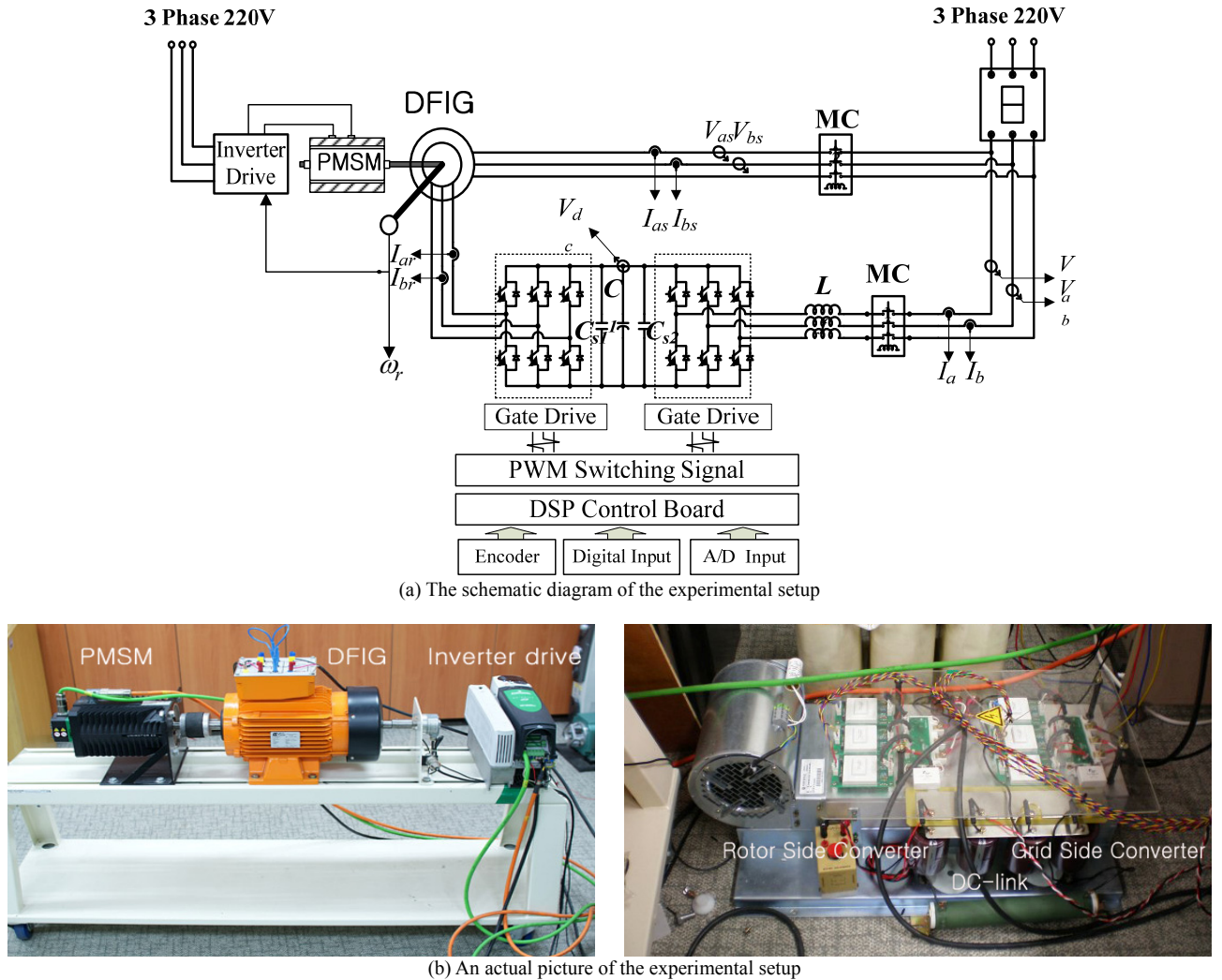


Fig. 7. The experimental setup of the DFIG system.

4. Simulation Results

Simulations were performed using PSIM to verify the proposed strategy. The proposed system was simulated as a rated 3 KW DFIG model. The parameters for the system are shown in Table 1. The detailed RSC and GSC models were constructed by switching the frequencies of both converters at 5 kHz. The grid voltage had an unsymmetrical condition; the a-phase had a value of 100%, the b-phase had a value of 100%, and the c-phase had a value of 90%.

The control strategies are illustrated in Figs. 4 and 5. Fig. 6 shows the simulation results, including the torque, DC-link voltage, the separated positive and negative currents, and the GSC currents. We observed the general steady states from 0.2—0.4 s. The unbalanced grid voltage was adapted to 0.4 s. The uncompensated control was applied from 0.4—0.7 s, and the RSC compensative control in the proposed strategy was applied from 0.7—1 s to reduce the torque ripple. From 1—1.2 s, the RSC and GSC control in the proposed strategy were both adapted to achieve the reduced ripple of the torque DC-link voltage.

Table 1. The Experimental Parameters

Rated Power	3[kW]
Number of pole pairs	4
Stator voltage	380[V]
Stator/rotor turns ratio	1.71875
R_s	0.61[Ω]
R_r	0.65[Ω]
L_s	67.6[mH]
L_r	67.6[mH]
L_m	63.9[mH]

5. Experimental Results

The experimental setup of the DFIG system is shown in Fig. 7. The rotor-side voltage source PWM converter was inserted into the rotor winding with the grid-side voltage source PWM converter connected to the stator winding via an AC filter. The converters were 3 kW-rated IGBT bridges with 2200 μ F DC-link capacitors. The sampling time was

100 μ s, and switching frequency was 5 kHz. The digital controller was based on a digital signal processor (TMS320VC33 DSP) and a 12-bit analog-to-digital (A/D) converter providing fast processing for the floating-point calculations.

Fig. 8 shows the grid-connecting process in the DFIG system [17]. MC1 was activated when the rotor speed reached a set rotor speed from 0—0.1 s. The d -axis current was controlled, allowing the magnitudes of the stator and grid voltage to be same from 0.1—0.18 s. The phase difference of the grid and stator was calculated from 0.18—0.38 s. Through the control of the q -axis current, the phase difference reached zero from 0.38—0.44 s. As the phase difference reached zero, the MC2 was activated in Fig. 8 (a), and the DFIG system was synchronized with the grid. There was a 10% voltage dip in one phase of the grid voltage (Fig. 9). The unbalanced grid voltage produced the ripple in the torque and the DC-link voltage.

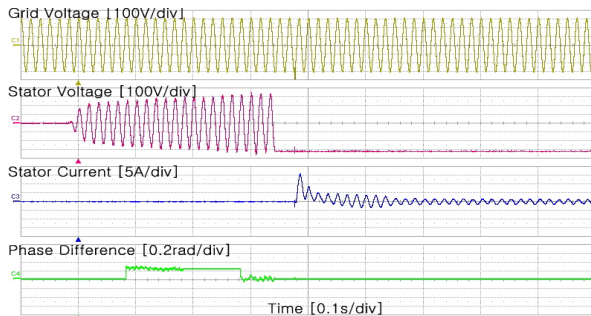


Fig. 8. The experimental results of the grid connections (a) Grid Voltage, (b) Stator Voltage, (c) Stator Current, and (d) Phase Difference between the grid and stator.

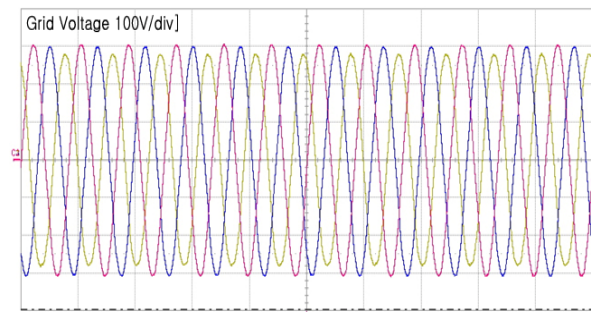


Fig. 9. The unbalanced grid voltage.

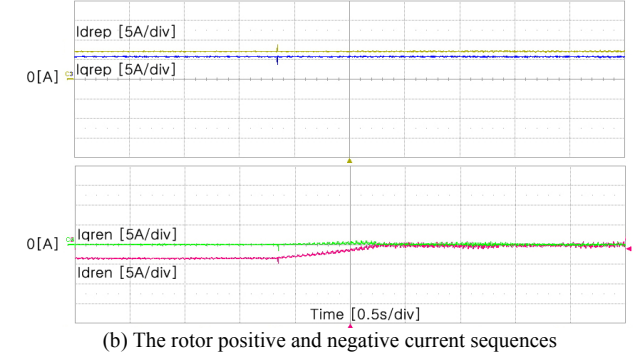
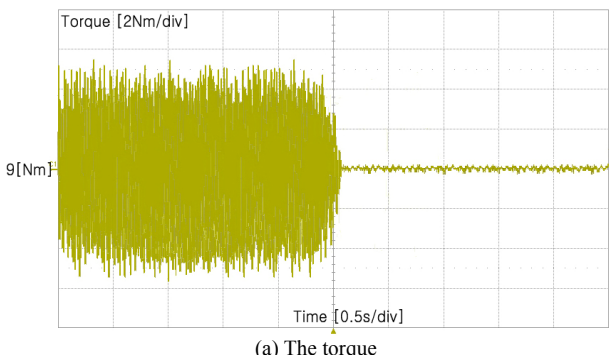


Fig. 10. The experimental results of the proposed RSC control method.

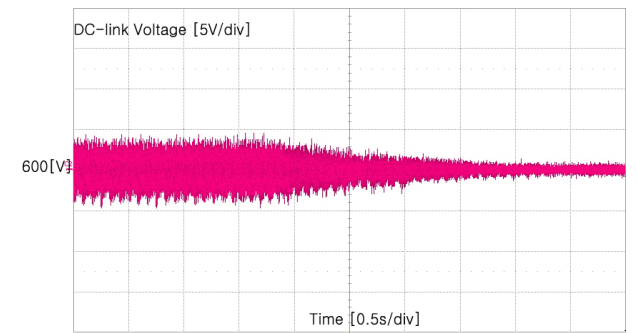


Fig. 11. The experimental results of the proposed GSC control method.

The torque ripple was reduced by controlling the positive and negative components of rotor current (Fig. 10). The positive and negative components of the rotor current were controlled, and the torque ripple was reduced at 2.5 s. Fig. 11 shows the reduction of DC-link voltage through the control of the GSC.

6. Conclusion

This paper has proposed a control method for reducing the DFIG torque and the ripple in the DC-link voltage under a grid voltage unbalance. RSC controlled the rotor negative sequence currents to eliminate any torque oscillation, whereas GSC controlled the DC-link voltage oscillation to ensure zero oscillation via the instantaneous power theory. The implementation results showed that the proposed control scheme improved the operating performance of the DFIG wind turbine system.

Acknowledgements

This work was supported by KESRI (2009T100100651), which is funded by MKE (Ministry of Knowledge Economy).

References

- [1] T. Ackermann, Wind Power in Power Systems, Vol. I. John Wiley and Sons, 2005, p. 58.
- [2] Yun-Seong Kim, Aditya Marathe, and Dong-Jun Won, "Comparison of Various Methods to Mitigate the Flicker Level of DFIG in Considering the Effect of Grid Conditions," *Journal of Power Electronics*, Vol. 9, No. 4, pp. 612-622, July. 2009.
- [3] Van-Tung Phan, Hong-Hee Lee, and Tae-Won Chun, "An Improved Control Strategy Using a PI-Resonant Controller for an Unbalanced Stand-Alone Doubly-Fed Induction Generator," *Journal of Power Electronics*, Vol. 10, No. 2, pp. 194-202, Mar. 2010.
- [4] D. Santos-Martin, J. L. Rodriguez-Amenedo, and S. Arnalte, "Direct Power Control Applied to Doubly Fed Induction Generator under Unbalanced Grid Voltage Conditions," *IEEE Trans. Power Electronics*, Vol. 23, No. 5, pp. 2328-2336, Sept. 2008.
- [5] A. Abo-Khalil, D. Lee, and J. Jang, "Control of back-to-back PWM converters for DFIG wind turbine systems under unbalanced grid voltage," in *Proc. IEEE ISIE*, pp. 2637-2642, 2007.
- [6] Patrick S. Flannery and G. Venkataraman, "Unbalanced Voltage Sag Ride-Through of a Doubly Fed Induction Generator Wind Turbine with Series Grid-Side Converter," *IEEE Trans. Industry Applications*, Vol. 45, No. 5, pp. 1879-1887, Sept. 2009.
- [7] T. Brekke and N. Mohan, "Control of a Doubly Fed Induction Wind Generator under Unbalanced Grid Voltage Conditions," *IEEE Trans. Energy Conversion*, Vol. 22, No. 1, pp. 129-135, Mar. 2007.
- [8] H. S. Song and K. Nam, "Dual current control scheme for PWM converter under unbalanced input voltage conditions," *IEEE Trans. Ind. Electronics*, Vol. 46, No. 5, pp. 953-959, Oct. 1995.
- [9] Gwi-Geun Park, Seon-Hwan Hwang, Jang-Mok Kim, Kyo-Beum Lee, and Dong-Choon Lee, "Reduction of Current Ripples due to Current Measurement Errors in a Doubly Fed Induction Generator," *Journal of Power Electronics*, Vol. 10, No. 3, pp. 313-319, May. 2010.
- [10] Sung-Tak Jou, Sol-Bin Lee, Yong Bae Park, and Kyo-Beum Lee, "Direct Power Control of a DFIG in Wind Turbines to Improve Dynamic Responses," *Journal of Power Electronics*, Vol. 9, No. 5, pp. 781-790, Sept. 2009.
- [11] Yi Zhou, P. Bauer, J. A. Ferreira, and J. Pierik, "Operation of Grid-Connected DFIG Under Unbalanced Grid Voltage Condition," *IEEE Trans. Energy Conversion*, Vol. 24, No. 1, pp. 240-246, Mar. 2009.
- [12] S. Djurovic, S. Williamson, and A. Renfrew, "Dynamic model for doubly-fed induction generators with unbalanced excitation, both with and without winding faults," *IET Electric Power Applications*, Vol. 3, No. 3, pp. 171-177, May. 2009.
- [13] F. M. Hughes, O. Anaya-Lara, N. Jenkins, and G. Strbac, "Dynamic Modeling and Control of DFIG-Based Wind Turbines under Unbalanced Network Conditions," *IEEE Trans. Power Systems*, Vol. 20, No. 4, pp. 1958-1966, Nov. 2005.
- [14] A. Tapia, G. Tapia, J. X. Ostolaza, and Jose Ramon Saenz, "Modeling and Control of a Wind Turbine Driven Doubly Fed Induction Generator," *IEEE Trans. Energy Conversion*, vol. 18, no. 2, pp. 194-204, June. 2003.
- [15] Y. Wang, L. Xu, and B. W. Williams, "Compensation of network voltage unbalance using doubly fed induction generator-based wind farms," *IET Renew Power Generation*, Vol. 3, No. 1, pp. 12-22, Mar. 2009.
- [16] Hea-Gwang Jeong, Kyo-Beum Lee, Sewan Choi, and Woojin Choi, "Performance improvement of LCL-filter based grid connected-inverters using PQR power transformations," *IEEE Trans. Power Electronics*, Vol. 25, No. 5, pp. 1320-1330, May. 2010.
- [17] J. Svensson and G. Saccoccando, "Transient operation of grid-connected voltage source converter under unbalanced voltage," in *Proc. Ind. Appl. Conf. 36th IAS Annu. Meeting*, 2001, Vol. 4, pp. 2419-2424.



Sol-Bin Lee was born in Jeonju, Korea in 1984. He received his B.S. in Electrical Engineering from Chonbuk National University, Korea and his M.S. in Electrical and Computer Engineering from Ajou University, Korea, in 2008 and 2010, respectively. His research interests include grid-connected systems and electric machine drives.



Kyo-Beum Lee was born in Seoul, Korea, in 1972. He received his B.S. and M.S. in Electrical and Electronic Engineering from the Ajou University, Korea in 1997 and 1999, respectively. He received his Ph.D. in Electrical Engineering from Korea University, Korea in 2003. From 2003 to 2006, he was with the Institute of Energy Technology, Aalborg University, Aalborg, Denmark. From 2006 to 2007, he was with the Division of Electronics and Information Engineering, Chonbuk National University, Jeonju, Korea. In 2007, he joined the School of Electrical and Computer Engineering, Ajou University, Suwon, Korea. He is an Associate Editor of the IEEE Transactions on Power Electronics and the Journal of Power Electronics. His current research interests include electric machine drives and wind power generation.



Dong-Choon Lee received his B.S., M.S., and Ph.D. in Electrical Engineering from Seoul National University, Seoul, Korea, in 1985, 1987 and 1993, respectively. He was a Research Engineer with Daewoo Heavy Industry from 1987 to 1988. Since 1994, he has been a faculty member of the Dept. of

Electrical Engineering, Yeungnam University, Gyeongbuk, Korea. Currently, he is a Full Professor at the College of Engineering. He is also serving as a Publication Editor in the Journal of Power Electronics, Korean Institute of Power Electronics, Korea. As a Visiting Scholar, he joined the Power Quality Laboratory, Texas A&M University, College Station (1998), the Electrical Drive Center, University of Nottingham, U.K. (2001), and the Wisconsin Electric Machines & Power Electronic Consortium, University of Wisconsin, Madison (2004). His current research interests include AC machine drives, control of power converters, wind power generation, and power quality.



Jang-Mok Kim was born in Busan, Korea in August 1961. He received his B.S. from Pusan National University in 1988, and his M.S. and Ph.D. in Electrical Engineering from Seoul National University, Korea in 1991 and 1996, respectively. From 1997 to 2000, he was a Senior Research Engineer with

the Korea Electrical Power Research Institute (KEPRI). Since 2001, he has been a faculty member of the School of Electrical Engineering, Pusan National University (PNU). In addition, he is a Research Member of the Research Institute of Computer Information and Communication at PNU. His present interests include the control of electric machines, electric vehicle propulsion, and power quality.